

Dear author,

Please note that changes made in the online proofing system will be added to the article before publication but are not reflected in this PDF.

We also ask that this file not be used for submitting corrections.



Contents lists available at ScienceDirect

International Journal of Heat and Mass Transfer

journal homepage: www.elsevier.com/locate/ijhmt

Nanoparticle layer detachment and its influence on the heat transfer characteristics in saturated pool boiling of nanofluids

Yosuke Watanabe, Koji Enoki, Tomio Okawa*

Department of Mechanical and Intelligent Systems Engineering, The University of Electro-Communications, 1-5-1, Chofugaoka, Chofu-shi, Tokyo 182-8585, Japan

ARTICLE INFO

Article history:

Received 12 January 2018

Received in revised form 14 March 2018

Accepted 16 April 2018

Available online xxxxx

Keywords:

Saturated pool boiling

Nanofluid

Nanoparticle layer

Peeling test

Adhesion force

Critical heat flux

Heat transfer coefficient

ABSTRACT

In nucleate pool boiling of nanofluid, nanoparticles suspended in liquid are deposited to form nanoparticle layer on the heated surface. As a result, surface properties are changed and the critical heat flux (CHF) is usually enhanced. However, since adhesion of the nanoparticle layer to the heated surface is not necessarily strong, partial detachment of the nanoparticle layer frequently occurs during nucleate boiling. In this study, peeling test was conducted for the nanoparticle layer formed during nucleate boiling of the water-based nanofluids to measure the adhesion force. The material of the heated surface was copper, and TiO_2 , Al_2O_3 and SiO_2 were used as the nanoparticle material. It was found that the adhesion force is highly dependent on the nanoparticle material; it was greatest for SiO_2 and weakest for TiO_2 in the present experiments. Then, saturated pool boiling curves were obtained using the damaged heated surfaces after the peeling. For the nanoparticle-layer coated surfaces without peeling, the heat transfer coefficient (HTC) was lower and CHF was higher than those for the bare surface. It was shown that with an increase in the mass of the nanoparticles removed by peeling, the decrease of HTC and the increase of CHF were mitigated. Even higher HTC values and a lower CHF value than those for the bare heated surface were measured for significantly damaged surfaces.

© 2018 Elsevier Ltd. All rights reserved.

1. Introduction

Nanofluid is the liquid in which nanometer-sized solid particles are suspended in a base liquid such as water or oil. It has been reported that in nucleate pool boiling in nanofluid, the heat transfer coefficient (HTC) and the critical heat flux (CHF) can significantly be different from those in the pure liquid containing no nanoparticles. Extensive reviews by several investigators showed that the HTC in nanofluids can be enhanced, deteriorated, or unchanged depending on the experimental conditions, whilst the CHF is usually enhanced greatly [1–9]. It is hence considered that boiling heat transfer of nanofluid can effectively be used for the cooling of high-power-density devices such as the next-generation CPU and the inverters for fuel-cell and electric vehicles [10,11]; it may also be applied to the emergency cooling of nuclear reactors [12,13].

During nucleate boiling in nanofluid, nanoparticles are deposited to form a thin layer on the heated surface. The formation of the nanoparticle layer is considered as a main mechanism causing the difference of the heat transfer characteristics since the surface

properties such as the roughness, the wettability and the wickability are totally changed [14–18]. For instance, Kim et al. [19] measured the contact angle of the nanoparticle-deposited heated surface to report that the contact angle decreased noticeably after the nucleate boiling in nanofluid and strong correlation was present between the surface wettability and the boiling heat transfer. Kim and Kim [20] showed that the CHF in the nanofluid can be correlated using the contact angle and the capillarity of the heated surface. It should however be noted that adhesion of the nanoparticle layer to the heated surface is not necessarily strong. Okawa et al. [21] found partial detachment of the TiO_2 nanoparticle layer from the heated surface during nucleate boiling in distilled water. They reported that the CHF enhancement by the nanoparticle layer was reduced when the nanoparticle layer detachment took place. Zuhairi et al. [22] also found the partial detachment of the nanoparticle layer for the TiO_2 - and SiO_2 -water nanofluids. Peculiar time-variation of the wall superheat was observed for these heated surfaces. It was discussed that such time-variation was related to the nanoparticle layer detachment. These experimental results show that the nanoparticle layer detachment may occur in the nucleate boiling of nanofluid and it can influence the boiling heat transfer characteristics.

Nanoparticles are not expensive and nanoparticle layer can easily be fabricated on the heated surface. It is hence expected that

* Corresponding author.

E-mail address: okawa.tomio@uec.ac.jp (T. Okawa).

Nomenclature

h	heat transfer coefficient
q_c	critical heat flux
q_w	wall heat flux
M	mass of nanoparticles remaining on the heated surface
M_0	total mass of nanoparticle layer
M_p	mass of nanoparticles peeled from the heated surface
F_{ad}	adhesion force
t_b	boiling time

Greek symbols

ΔT_w	wall superheat
θ	contact angle

Subscript

mean	mean value
------	------------

Other notation

CV(x)	cumulative value of x
-------	-----------------------

the nanoparticle-deposited surface can be used as the enhanced heat transfer surface of economic advantage. However, sufficiently tight adhesion is required for the nanoparticle layer in this case. Also, in the application to the emergency cooling of nuclear reactor, temporary change of the heat transfer characteristics may lead to unexpected outcome. However, no quantitative experimental information is available for the adhesion force of the nanoparticle layer and the influence of the nanoparticle layer detachment on the boiling heat transfer characteristics. In view of this, in this work, peeling test is conducted for the nanoparticle layers formed on the heated surface. As the typical materials, copper is used as the material of the heated surface and titanium-dioxide (TiO_2), alumina (Al_2O_3), and silica (SiO_2) are used as the nanoparticle material. Using the damaged heated surface after peeling, boiling curves are obtained to investigate the influence of the nanoparticle layer detachment on the HTC and CHF in the nucleate pool boiling of distilled water.

2. Experimental method**2.1. Experimental apparatus**

Photograph and schematic diagram of the experimental apparatus are depicted in Fig. 1(a) and (b), respectively. The copper block containing nine cartridge heaters was set on the bottom plate of the cylindrical experimental vessel. The end face of the copper block of 20 mm in diameter was used as the heated surface. Each cartridge heater was 7.3 mm in diameter and 45 mm in length, and its maximum power was 100 W. The maximum achievable heat flux is hence calculated 2.87 MW/m^2 ; the power of the cartridge heaters was controlled using a volt slider. To reduce the heat loss from the side wall of the copper block, it was covered by the stainless steel jacket and the space between the copper block and the jacket was filled with glass wool. The copper block and the jacket were bonded smoothly by means of electron beam welding. The copper block contained four calibrated type-K thermocouples accurate to within ± 0.1 – 0.3 K on the central axis to calculate the wall superheat ΔT_w and the heat flux q_w and to shut down the system when the CHF condition was reached. From the error propagation analyses, the measurement uncertainties of ΔT_w and q_w were estimated within $\pm 2 \text{ K}$ and $\pm 58 \text{ kW/m}^2$, respectively.

The experimental vessel was 144 mm in diameter and 170 mm in height; it was mainly made of transparent polycarbonate but the bottom plate was made of stainless steel. The elevation of the heated surface was 35 mm from the bottom of the vessel and the water level was 110 mm as shown in Fig. 1. During the experiments reported in this paper, the side wall of the vessel was covered with a thermal insulation material to reduce the heat loss. The immersion heater in the vessel was used to heat up the sub-cooled liquid and then maintain the liquid temperature at the saturation temperature. The liquid temperature was measured 10

mm above the heated surface using a type-K thermocouple accurate to within $\pm 0.3 \text{ K}$. A Dimroth condenser was equipped on the top lid of the vessel to keep the mass of test liquid in the vessel constant. Since the vessel was open to the atmosphere through the condenser, the pressure in the vessel was close to the atmospheric pressure.

2.2. Formation of the nanoparticle layer on the heated surface

As the material of nanoparticles, TiO_2 (Aeroxide TiO_2 P25; mixture of 80% anatase and 20% rutile), Al_2O_3 (Aeroxide Alu C), and SiO_2 (Aeroxide 90 G) were used. To prepare the nanofluid, 300 mg of nanoparticles were weighed using an electronic balance accurate to within $\pm 0.07 \text{ mg}$ (HR-202i, A&D Co., Ltd.). The weighed nanoparticles were then mixed with 200 ml of distilled water and ultrasonic excitation at 430 kHz was performed for 3 h using an ultrasonic bath (QR-003, Kaijo Co., Ltd.). These procedures were considered sufficient to ensure stable particle dispersion since no noticeable particle sedimentation was found even 24 h after the nanofluid preparation. Fig. 2 shows the particle size distributions in the nanofluids that were measured using a particle diameter analyzer (FPAR-1000, Otsuka Electronics Co, Ltd.). It can be seen that the particle size distributed within 80–800 nm and greater than the mean primary particle sizes reported by the manufacturer (21 nm for TiO_2 , 13 nm for Al_2O_3 , and 20 nm for SiO_2); this results suggest that nanoparticles formed clusters in the nanofluids [14,15]. After preparing the nanofluid, the heated surface was polished using metal polishing paste and cleaned using acetone. The surface wettability was then measured using a contact angle goniometer (PG-X, Fibro System AB) to confirm that the contact angle was within the prescribed range of $90 \pm 5^\circ$.

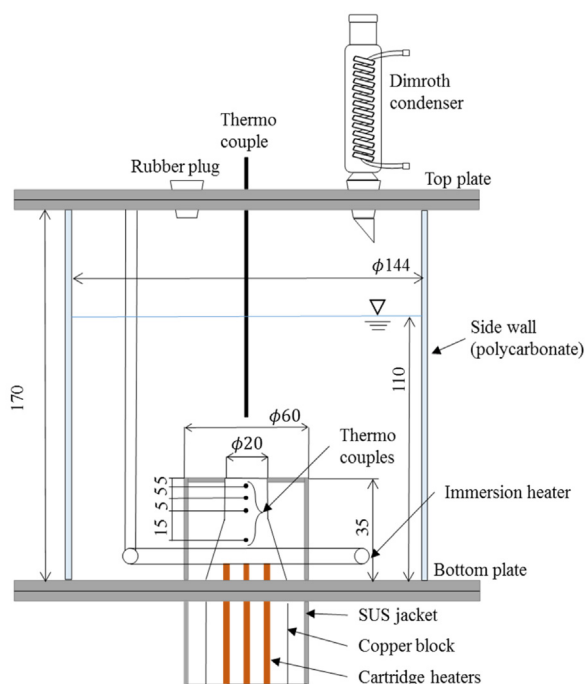
After setting the heating device on the experimental vessel, 1300 ml of distilled water was supplied and saturated pool boiling was initiated in the vessel using the heating device and the immersion heater; here, the heat flux of the heating device q_w was set at 650 kW/m^2 . After keeping saturated boiling for about 20 min for degassing, 200 ml of nanofluid was added to the test liquid. Since 300 mg of nanoparticle was contained, the nanoparticle concentration of the test liquid was calculated 0.2 kg/m^3 . Nucleate boiling was maintained for 60 min to form the nanoparticle layer on the heated surface. The photographs of the original bare surface and the 3 nanoparticle-layer coated surfaces are presented in Fig. 3 (a)–(d), respectively. Appearance of the Al_2O_3 nanoparticle-deposited surface (Fig. 3(c)) was relatively similar to that of the original surface (Fig. 3(a)), but the TiO_2 and SiO_2 nanoparticle-deposited surfaces (Fig. 3(b) and (d)) were whitish in color.

2.3. Experimental procedure

As shown in Fig. 4, the following three types of measurement were performed after the preparation of the nanoparticle-



(a) Photo



(b) Schematic diagram (scale size [mm])

Fig. 1. Experimental apparatus.

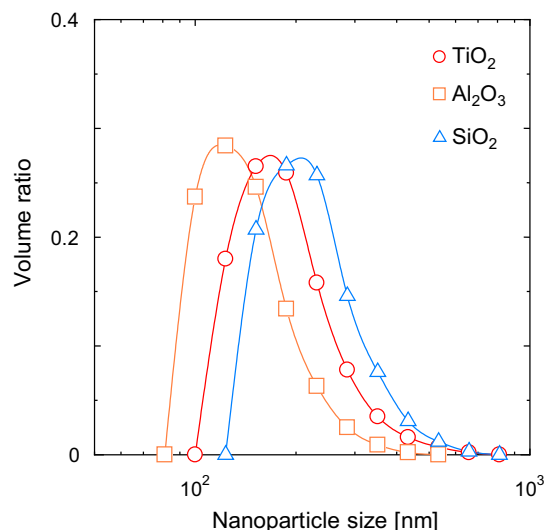


Fig. 2. The nanoparticle size distribution in nanofluids (volume ratio).

In the first experiment, the nanoparticles deposited on the heated surface was scraped off using a plastic spatula and the total mass M_0 was weighed using the electronic balance.

In the second experiment, peeling test was carried out using four adhesive tapes of different adhesive forces (4, 11.5, 22, and 40 N for the tape of 10 mm width measured under JIS (Japanese Industrial Standards) Z 0237 [23]). In JIS Z 0237, it is stipulated that a 100 mm long adhesive tape is applied on a clean stainless steel surface and one end of the tape is pulled slowly in the perpendicular direction to the surface to measure the tensile force. It should hence be noted that the surface condition stipulated in JIS is quite different from that in the present experiment. Detailed experimental procedure is described as follows.

1. An adhesive tape was weighed and then applied to the nanoparticle-deposited surface (the weakest tape was used first).
2. After 5 min, the tape was peeled away slowly in the vertical direction; the tensile strength was measured using a force gage (ZTS-50N, Imada Co., Ltd.) since the adhesion force of the tape to the nanoparticle layer F_{ad} was unknown. The force gage was accurate to within ± 0.11 N.
3. The tape was weighed again to calculate the mass of removed nanoparticles from the weight difference of the tape. Using the new tape of same adhesion force, the steps 1 to 3 were repeated until no nanoparticles were removed in the peeling test.
4. Using the tape of stronger adhesion force, the steps 1 to 3 were carried out again.
5. After completing the measurements using all the four tapes, the nanoparticles still remaining on the heated surface was scraped off to measure the total mass of the deposited nanoparticles using the electronic balance.

In the above procedure, the cumulative mass of the removed nanoparticles increased with an increase in the adhesion force of the tape. The photographs of the heated surface at several peeling levels are presented in Fig. 5; here, M/M_0 denotes the ratio of the nanoparticles remaining on the heated surface. The state of the nanoparticle layer is not visible for Al₂O₃, but it can be seen that for TiO₂, removal of the nanoparticle layer occurred inhomogeneously on the heated surface. For SiO₂, the adhesion force was relatively large and no noticeable nanoparticle layer detachment occurred in the present experiment.

deposited surface: (1) measurement of the total mass of the nanoparticle layer, (2) measurement of the adhesion force of the nanoparticle layer, and (3) measurement of the boiling heat transfer characteristics (HTC and CHF) for the damaged heated surface.

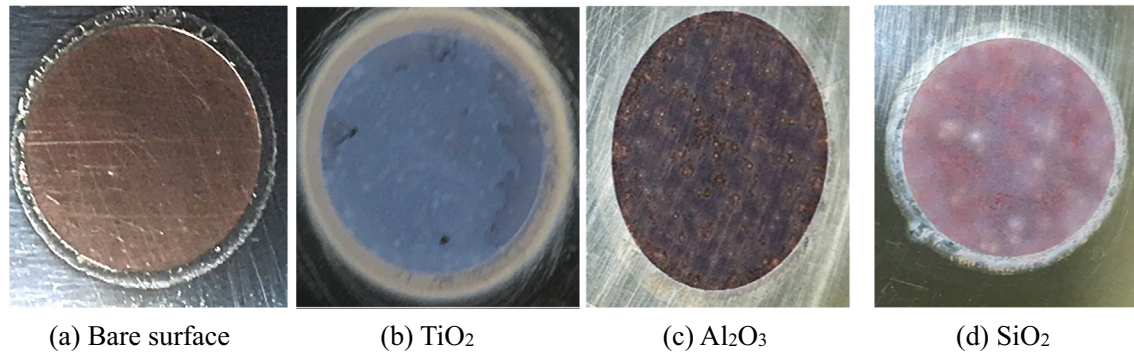


Fig. 3. Appearances of the heated surface before and after the nanoparticle deposition.

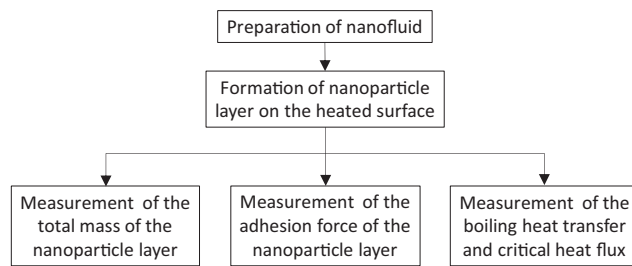


Fig. 4. Flowchart of experimental procedure.

mean values of M_0 are presented in Fig. 6; here, the error bars refer to the minimum and maximum values of M_0 measured in the present experiment. The figure indicates that the mean value of M_0 was 1.05 mg for TiO_2 , 0.51 mg for Al_2O_3 , and 0.23 mg for SiO_2 . Reproducibility of the experiment is considered satisfactory since the scattering of M_0 for each material was within $\pm 10\%$ of the mean value. It can be seen that the nanoparticle deposition was greatest for TiO_2 whilst least for SiO_2 . The value of M_0 for TiO_2 is 4.6 times the value for SiO_2 , indicating that the effect of the nanoparticle material on M_0 is significant.

3.2. Adhesion force of nanoparticle layer

In Fig. 7, the mass of the nanoparticles removed in each peeling test M_p is plotted against the peeling time. Here, as a typical example, the results for the case that the nanoparticle material was TiO_2 and tape's adhesive force was 11.5 N under JIS Z 0237 are shown. In the figure, the cumulative value of M_p ($\text{CV}(M_p)$) is also plotted. As shown in the figure, most nanoparticles were removed in the first peeling and M_p became zero at the third peeling; the tendency was similar in all the cases. The difference of M_0 and $\text{CV}(M_p)$ when M_p became zero was regarded as M that is the mass of the nanoparticles deposited to the heated surface with the adhesion force greater than F_{ad} .

The mass ratio of the nanoparticles remaining on the heated surface M/M_0 is plotted against the adhesion force F_{ad} in Fig. 8. In the case of TiO_2 , the value of M/M_0 decreases rapidly from 0.84 to 0.28 with the increase of F_{ad} from 1.9 to 2.8 N. If the value of F_{ad} at which $M/M_0 = 0.5$ is defined as the mean adhesion force of nanoparticles $F_{ad,mean}$, the value of $F_{ad,mean}$ is estimated about 2.4 N for TiO_2 . Similarly, $F_{ad,mean}$ is estimated about 4.9 N for Al_2O_3 . For SiO_2 , $F_{ad,mean}$ is greater than 4.6 N but the exact value is unknown since only 9% of nanoparticles were removed even when the strongest adhesion tape was used. These results indicate that the adhesion force of the nanoparticles is dependent significantly on the particle material. Under the present experimental condition, the order of the adhesion strength is $\text{SiO}_2 > \text{Al}_2\text{O}_3 > \text{TiO}_2$.

It should be noted that in Fig. 6, the total mass of the deposited nanoparticles was in the reverse order ($\text{TiO}_2 > \text{Al}_2\text{O}_3 > \text{SiO}_2$). Hence, there is a possibility that the total mass of the nanoparticles deposited on the heated surface is one of the important factors causing the difference of adhesion strength. Thus, the boiling time in the nanofluid was shortened from 60 min to 5 min to carry out the same experiments. In this case, M_0 decreased from 1.05 mg to 0.40 mg for TiO_2 , from 0.51 mg to 0.35 mg for Al_2O_3 , and from 0.23 mg to 0.27 mg for SiO_2 . The value of M_0 decreased for TiO_2 and Al_2O_3 whilst increased slightly for SiO_2 . It is hence considered that in the case of SiO_2 , M_0 already reached the equilibrium value within 5 min. The results of peeling test when the boiling time

In the third experiment, the heated surfaces at several peeling levels were set on the experimental vessel to measure the boiling heat transfer characteristics. It is noted that in this experiment, distilled water was used as the test liquid to avoid further deposition of nanoparticles. The experimental procedure is described as follows.

1. The heating device was set and the experimental vessel was filled with 1500 ml of distilled water.
2. Nucleate boiling was elicited in the vessel as in the preparation of the nanoparticle-deposited surface: the value of q_w was kept at 650 kW/m^2 to maintain saturated nucleate boiling for 20 min for degassing.
3. The heat flux q_w was then increased step by step. The increment of q_w in each step was less than 50 kW/m^2 . Usually, the copper block temperature increased gradually with an increase in q_w . When sudden rise of the copper block temperature was detected, the cartridge heaters were shut down and the value of q_w just before the sudden temperature rise was regarded as the CHF. Usually, it took about 80 min in this experimental step. During each experimental run, the temperature data were recorded every one second using a data acquisition system.

Here, it should be noted that nanoparticle layer detachment may occur during the measurement of the boiling heat transfer characteristics to affect the measured boiling curves. However, since no significant nanoparticle layer detachment was found even after the CHF measurement, it was assumed that the effect of the nanoparticle layer detachment during the measurement of the boiling heat transfer characteristics was fairly small in the present experiments.

3. Results and discussion

3.1. Total mass of nanoparticle layer

In the first experiment, the total mass of the nanoparticle layer M_0 was measured three times for each nanoparticle material. The

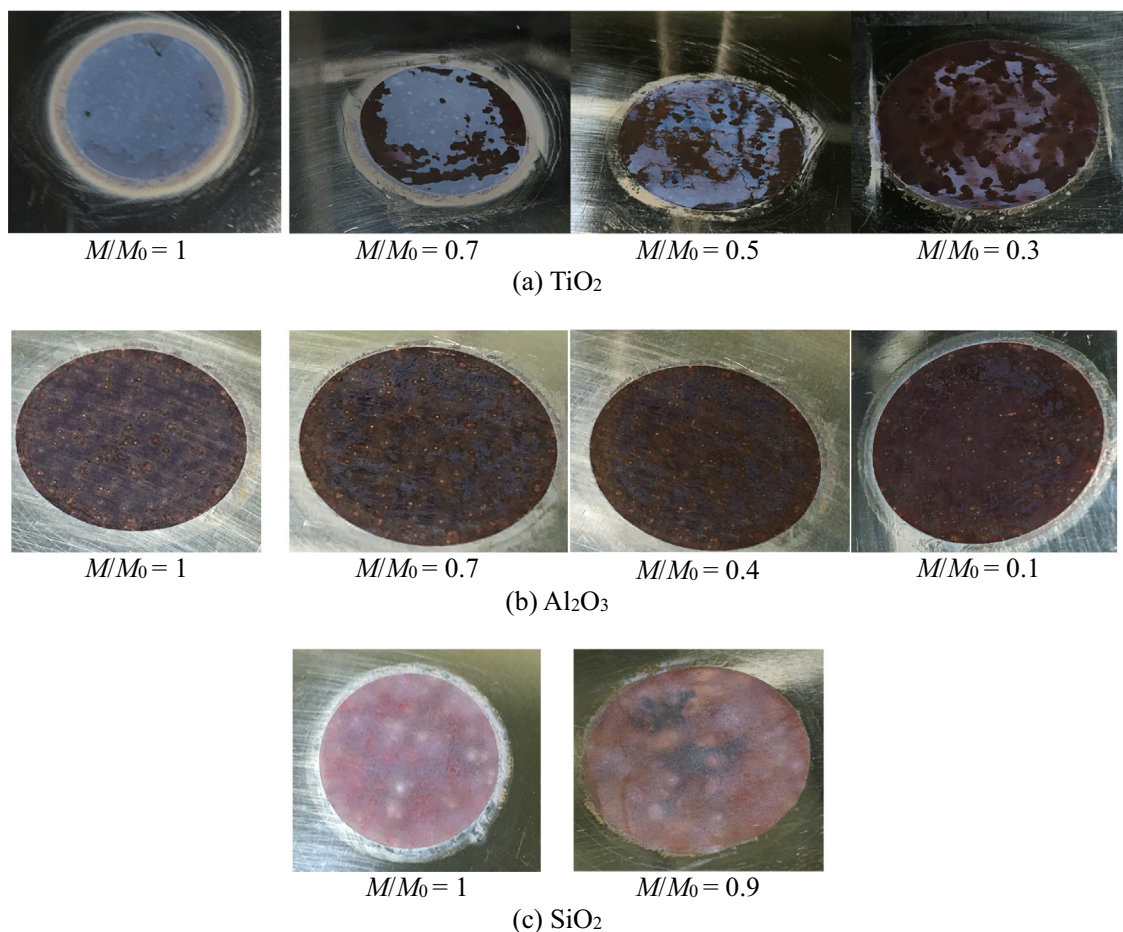


Fig. 5. Appearance of the heated surface at several peeling levels.

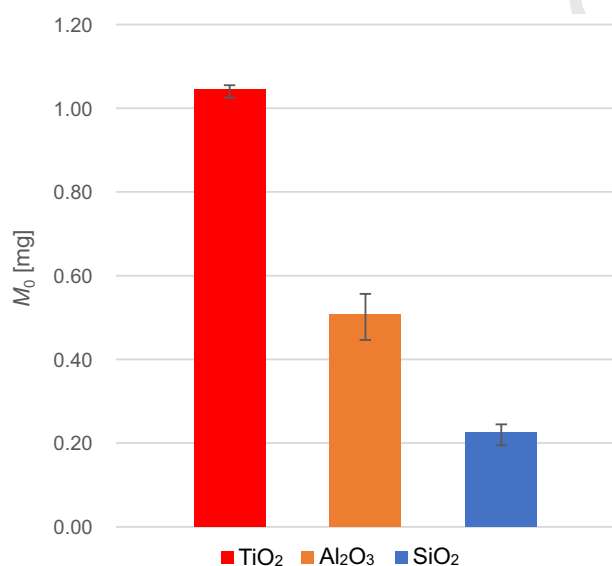


Fig. 6. Total mass of the nanoparticle layer formed on the heated surface (M_0).

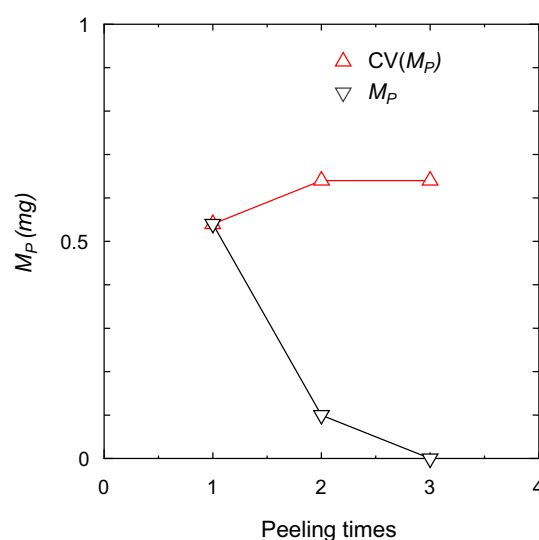


Fig. 7. Relationship between the peeling times and the mass of removed nanoparticles (nanoparticle material is TiO_2 and the tape's adhesive force is 11.5 N under JIS).

was shortened are presented with the dashed lines in Fig. 8 (the value of M_0 in each experimental condition is listed in Table 1). In the cases of TiO_2 and Al_2O_3 , the decrease of M_0 led to the slight increase of $F_{ad,mean}$, suggesting that the adhesion force is dependent on the amount of deposited nanoparticles. However, the effect

of nanoparticle material is more significant in Fig. 8. It is hence confirmed that the adhesion force is primarily influenced by the particle material.

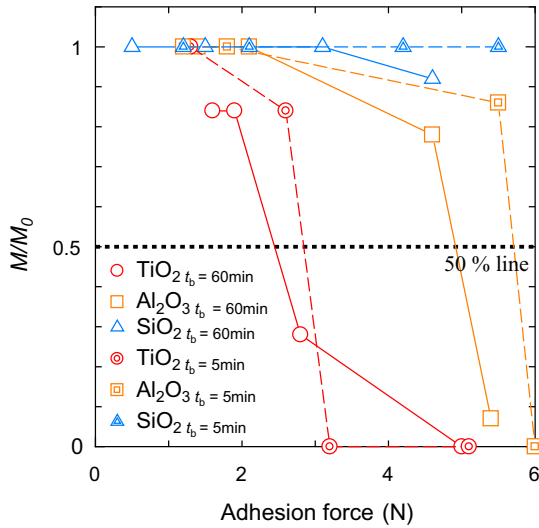


Fig. 8. Adhesion force of the nanoparticle layer.

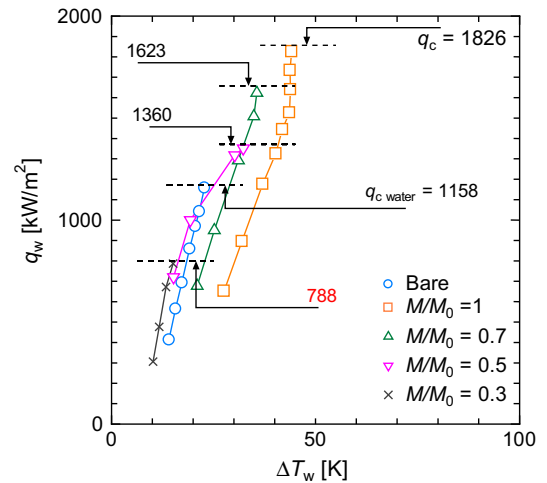
3.3. Boiling heat transfer characteristics (HTC and CHF)

Presented in Fig. 9 are the boiling curves obtained using the heated surfaces of various peeling levels. First, it can be seen in Fig. 9(c) that for the bare surface, the HTC agreed with the Stephan-Abdelsalam correlation [24] fairly well and the measured CHF value (1.16 MW/m²) was close to that calculated by Zuber's correlation (1.11 MW/m²) [25].

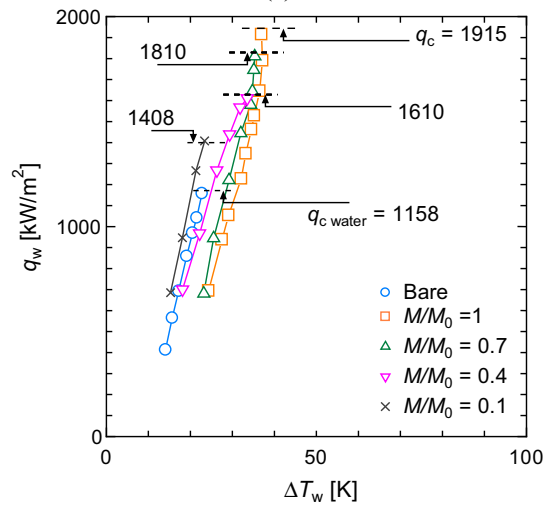
For the non-damaged nanoparticle-deposited surfaces ($M/M_0 = 1$), ΔT_w increased 8–15 K and CHF increased to 1.82–1.92 MW/m², depending on the nanoparticle material. The deterioration of HTC was most significant for TiO₂ in which the total mass of the deposited nanoparticles was largest (see Fig. 6), suggesting that the boiling heat transfer was deteriorated since the nanoparticle layer acted as the thermal insulation material. Whilst, the CHF values for nanoparticle-deposited surfaces were about 1.6 times the value for the bare surface and the influence of the nanoparticle material was not noticeable.

To investigate the effect of the nanoparticle-layer detachment on boiling HTC, the values of HTC at the heat flux of $q_w = 700$ W/m² are plotted against M/M_0 in Fig. 10. It can be seen that the deterioration of HTC was mitigated with the progress of nanoparticle layer detachment, supporting the hypothesis that the nanoparticle layer acted as the thermal insulation material. It may be interesting to note that the HTC values for significantly damaged surfaces were even greater than that for the bare surface.

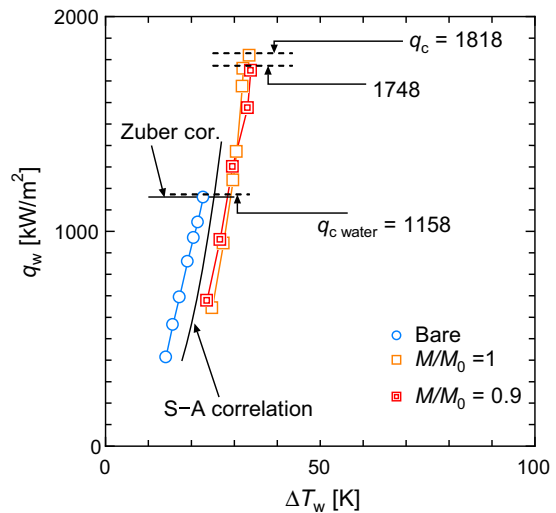
The CHF values q_c are plotted against M/M_0 in Fig. 11. It can be seen that CHF decreases monotonically with decreased value of M/M_0 and even the CHF value smaller than that for the bare surface was measured for the most damaged surface of TiO₂ ($M/M_0 = 0.3$). Since the CHF is usually enhanced for the hydrophilic surface, the dependence of the contact angle θ on M/M_0 is explored in Fig. 12. In the measurement of θ , droplets were placed at arbitrary three different positions on the heated surface. In several cases, θ could not be measured since the droplet was completely absorbed



(a) TiO₂



(b) Al₂O₃



(c) SiO₂

Fig. 9. Boiling curves (unit of CHF is kW/m²).

Table 1
Relationship between the boiling time (t_b) and M_0 .

	M_0 ($t_b = 60$ min) [mg]	M_0 ($t_b = 5$ min) [mg]
TiO ₂	1.05	0.40
Al ₂ O ₃	0.51	0.35
SiO ₂	0.23	0.27

into the nanoparticle layer. In this case, the value of θ was assumed to be zero in Fig. 12. It can be seen that the value of θ was small for the non-damaged surfaces ($M/M_0 = 1$) and tended to increase with the progress of the nanoparticle layer detachment. This trend is

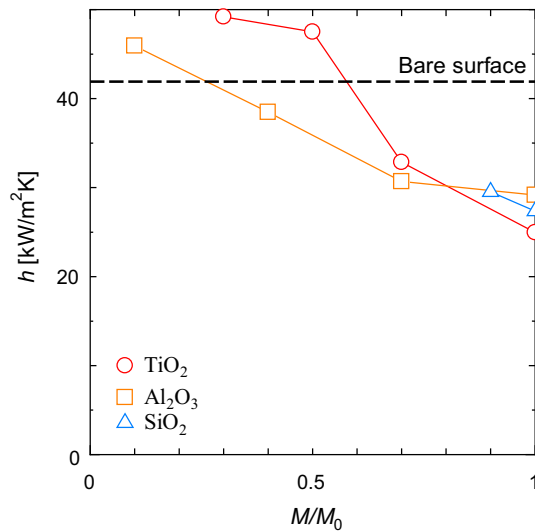


Fig. 10. Heat transfer coefficients (HTCs) for the nanoparticle-layer deposited surfaces at various detachment level ($q_w = 700 \text{ kW/m}^2 \text{ K}$).

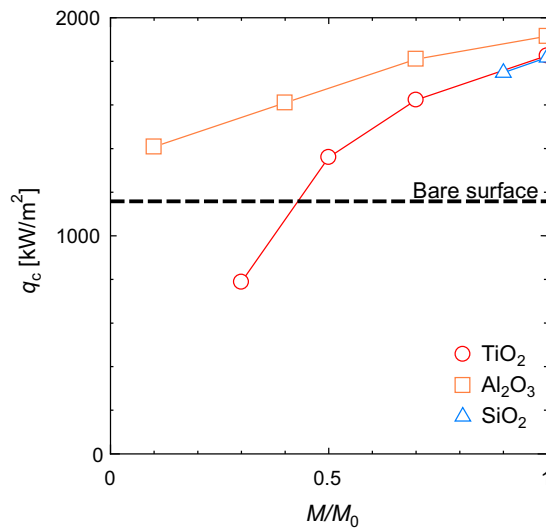


Fig. 11. Critical heat fluxes (CHF) for the nanoparticle-layer deposited surfaces at various detachment level.

consistent with the dependence of CHF on M/M_0 , suggesting that improvement of the surface wettability is one the main causes of the CHF enhancement. Significant scattering of θ is seen for several damaged surfaces (e.g. $M/M_0 = 0.3$ for TiO_2 and $M/M_0 = 0.4$ for Al_2O_3). This is considered to reflect the fact that the nanoparticle layer detachment was inhomogeneous as delineated in Fig. 5.

From the present results, it is considered that nanoparticle-layer's acting as a thermal insulation material and the improvement of the surface wettability are main causes of the deterioration of the boiling heat transfer and the CHF enhancement, respectively. However, these factors do not describe the larger HTC and the smaller CHF than those for the bare surface measured for significantly damaged surfaces. Since the nanoparticle-layer detachment was inhomogeneous, it is inferred that peculiar boiling occurred at the edge of the remaining nanoparticle layer to cause the increase of HTC and the decrease of CHF.

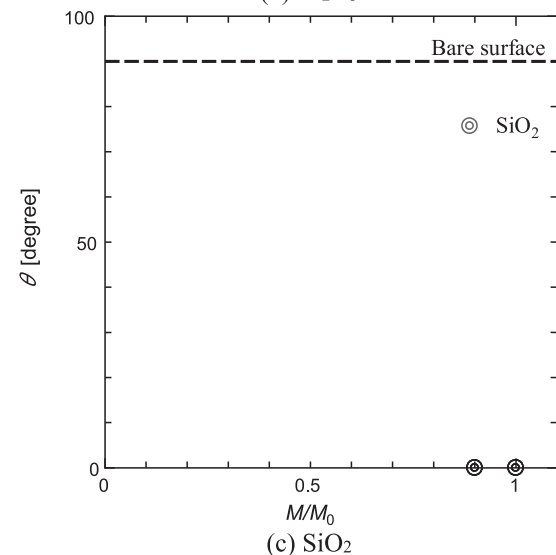
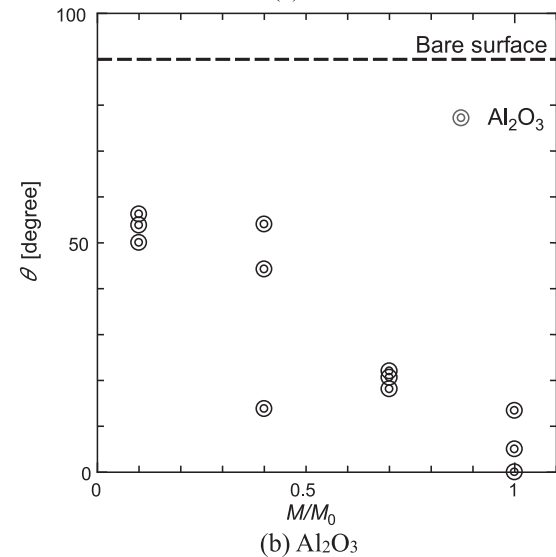
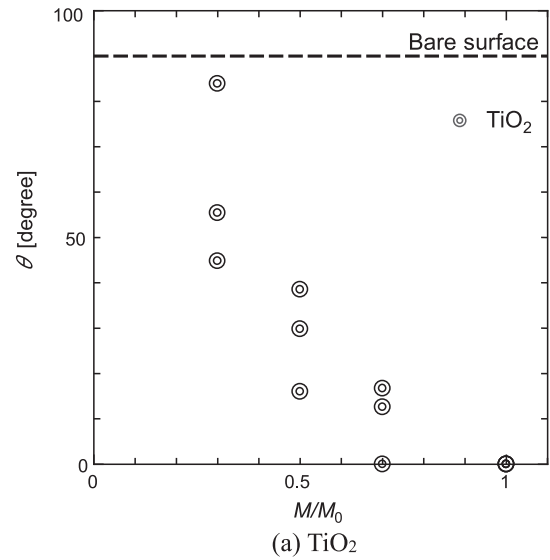


Fig. 12. Contact angles of the nanoparticle-layer deposited surfaces at various detachment level.

4. Conclusion

In nucleate boiling of nanofluid, nanoparticle layer is formed on the heated surface to influence the heat transfer coefficient and the critical heat flux. In this work, experiments were conducted to investigate the adhesion force of the nanoparticle layer to the heated surface and the effect of nanoparticle layer detachment on the boiling heat transfer characteristics. The main results obtained in this study are summarized as follows.

- It was found that the total mass of the nanoparticles deposited on the heated surface and the adhesion force of the nanoparticle-layer were dependent significantly on the nanoparticle material. Under the experimental conditions of this work, the mass of the deposited nanoparticles was in the order of $\text{TiO}_2 > \text{Al}_2\text{O}_3 > \text{SiO}_2$ and the adhesion force was in the order of $\text{SiO}_2 > \text{Al}_2\text{O}_3 > \text{TiO}_2$.
- The nanoparticle layer formed on the heated surface acted as a thermal insulation material and improved surface wettability. As a result, boiling heat transfer was deteriorated but the critical heat flux was enhanced for the nanoparticle-deposited surfaces. Deterioration of boiling heat transfer was most significant for TiO_2 in which the mass of deposited nanoparticles was largest. Whilst, the effect of nanoparticle material on the critical heat flux enhancement was not noticeable.
- With removal of the nanoparticle-layer, the mass of the deposited nanoparticles decreased and the surface contact angle increased. As a result, the deterioration of the boiling heat transfer and the enhancement of the critical heat flux were reduced with the progress of the nanoparticle-layer detachment level. Even the larger heat transfer coefficients and the smaller critical heat flux than those for the bare heated surface were measured for significantly damaged surfaces. In the present experiments, nanoparticle-layer detachment occurred inhomogeneously. It was hence discussed that peculiar boiling at the edge of the remaining nanoparticle layer contributed to the increase of HTC and the decrease of CHF.

Conflict of interest

The authors declare that there are no conflict of interest.

Acknowledgement

This work was supported by KAKENHI (No. 26420140).

References

- [1] R. Kamatchi, S. Venkatachalapathy, Parametric study of pool boiling heat transfer with nanofluids for the enhancement of critical heat flux: a review, *Int. J. Therm. Sci.* 87 (2015) 228–240.

- [2] H. Kim, Enhancement of critical heat flux in nucleate boiling of nanofluids: a state-of-art review, *Nanoscale Res. Lett.* 6 (2011) 415.
- [3] S.M. Sohel Murshed, C.A. Nieto de Castro, M.J.V. Lourenço, M.L.M. Lopes, F.J.V. Santos, A review of boiling and convective heat transfer with nanofluids, *Renew. Sustain. Energy Rev.* 15 (5) (2011) 2342–2354.
- [4] J. Barber, D. Brutin, L. Tadrist, A review on boiling heat transfer enhancement with nanofluids, *Nanoscale Res. Lett.* 6 (2011) 280.
- [5] S.M. You, M. Amaya, S.M. Kwark, A review of enhancement of boiling heat transfer through nanofluids and nanoparticle coatings, *Int. J. Air-Cond. Refrig.* 18 (4) (2010) 247–263.
- [6] R.A. Taylor, P.E. Phelan, Pool boiling of nanofluids: comprehensive review of existing data and limited new data, *Int. J. Heat Mass Transf.* 52 (23–24) (2009) 5339–5347.
- [7] L. Cheng, E.P. Bandarra Filho, J.R. Thome, Nanofluid two-phase flow and thermal physics: a new research frontier of nanotechnology and its challenges, *J. Nanosci. Nanotechnol.* 8 (2008) 3315–3332.
- [8] L. Godson, B. Raja, D. Mohan Lal, S. Wongwises, Enhancement of heat transfer using nanofluids-an overview, *Renew. Sustain. Energy Rev.* 14 (2010) 629–641.
- [9] Y. Li, J. Zhou, S. Tung, E. Schneider, S. Xi, A review on development of nanofluid preparation and characterization, *Powder Technol.* 196 (2009) 89–101.
- [10] M. Rafiqul Islam, B. Shabani, G. Rosengarten, Nanofluids to improve the performance of PEM fuel cell cooling systems: a theoretical approach, *Appl. Energy* 178 (2016) 660–671.
- [11] D.P. Kulkarni, R.S. Vajha, D.K. Das, Application of aluminum oxide nanofluids in diesel electric generator as jacket water coolant, *Appl. Therm. Eng.* 28 (2008) 1774–1781.
- [12] S. Kim, H.D. Kim, H. Kim, H.S. Ahn, H. Jo, J. Kim, M.H. Kim, Effects of nano-fluid and surfaces with nano structure on the increase of CHF, *Exp. Therm. Fluid Sci.* 34 (2010) 487–495.
- [13] I.C. Bang, G. Heo, Y.H. Jeong, S. Heo, An axiomatic design approach of nanofluid-engineered nuclear safety features for generation III+ reactors, *Nucl. Eng. Technol.* 41 (2009) 1157–1170.
- [14] I.C. Bang, S.H. Chang, Boiling heat transfer performance and phenomena of Al_2O_3 -water nano-fluids from a plain surface in a pool, *Int. J. Heat Mass Transf.* 48 (2005) 2407–2419.
- [15] H.D. Kim, J. Kim, M.H. Kim, Experimental studies on CHF characteristics of nano-fluids at pool boiling, *Int. J. Multiph. Flow* 33 (2007) 691–706.
- [16] S.J. Kim, I.C. Bang, J. Buongiorno, L.W. Hu, Surface wettability change during pool boiling of nanofluids and its effect on critical heat flux, *Int. J. Heat Mass Transf.* 50 (2007) 4105–4116.
- [17] S.J. Kim, I.C. Bang, J. Buongiorno, L.W. Hu, Effects of nanoparticle deposition on surface wettability influencing boiling heat transfer in nanofluids, *Appl. Phys. Lett.* 89 (2006) Article No. 153107.
- [18] G. Dewitt, T. McKrell, J. Buongiorno, L.W. Hu, R.J. Park, Experimental study of critical heat flux with alumina-water nanofluids in downward facing channels for in-vessels retention applications, *Nucl. Eng. Technol.* 45 (3) (2013) 335–346.
- [19] H. Kim, J. Kim, M.H. Kim, Effect of nanoparticles on CHF enhancement in pool boiling of nano-fluids, *Int. J. Heat Mass Transf.* 49 (2006) 5070–5074.
- [20] H.D. Kim, M.H. Kim, Effect of nanoparticle deposition on capillary wicking that influences the critical heat flux in nanofluids, *Appl. Phys. Lett.* 91 (2007) Article No. 014104.
- [21] T. Okawa, M. Takamura, T. Kamiya, Boiling time effect on CHF enhancement in pool boiling of nanofluids, *Int. J. Heat Mass Transf.* 55 (2012) 2719–2725.
- [22] M. Zuhairi Sulaiman, D. Matsuo, K. Enoki, T. Okawa, Systematic measurements of heat transfer characteristics in saturated pool boiling of water-based nanofluids, *Int. J. Heat Mass Transf.* 102 (2016) 264–276.
- [23] Japanese Industrial Standards, Testing methods of pressure-sensitive adhesive tapes and sheets, *JIS Z 0237* (2009).
- [24] K. Stephan, M. Abdelsalam, Heat-transfer correlations for natural convection boiling, *Int. J. Heat Mass Transf.* 23 (1980) 73–87.
- [25] N. Zuber, M. Tribus, J. W. Westwater, The hydrodynamic crisis in pool boiling of saturated and subcooled liquids, in: *Proceedings of the 2nd International Heat Transfer Conference*, Boulder, Colorado, 1961, pp. 230–236.